SCIENTIFIC REPORTS

OPEN

SUBJECT AREAS:
APPLIED PHYSICS
COMPUTATIONAL METHODS
ELECTRONIC DEVICES
PHASE TRANSITIONS AND CRITICAL PHENOMENA

Received
18 June 2013

Accepted
2 September 2013

Published
24 September 2013

Correspondence and requests for materials should be addressed to S.K.L. (linsk@mail.ncku.edu.tw)

Ab initio-aided CALPHAD thermodynamic modeling of the Sn-Pb binary system under current stressing

Shih-kang Lin[1,2,3], Chao-kuei Yeh[1], Wei Xie[4], Yu-chen Liu[1] & Masahiro Yoshimura[1,2]

[1]Department of Materials Science and Engineering, National Cheng Kung University, Tainan city 70101, TAIWAN, [2]Promotion Center for Global Materials Research, National Cheng Kung University, Tainan city 70101, TAIWAN, [3]Center for Micro/Nano Science and Technology, National Cheng Kung University, Tainan city 70101, TAIWAN, [4]Department of Materials Sciences and Engineering, University of Wisconsin – Madison, Madison, WI 53706, USA.

Soldering is an ancient process, having been developed 5000 years ago. It remains a crucial process with many modern applications. In electronic devices, electric currents pass through solder joints. A new physical phenomenon – the supersaturation of solders under high electric currents – has recently been observed. It involves (1) un-expected supersaturation of the solder matrix phase, and (2) the formation of unusual "ring-shaped" grains. However, the origin of these phenomena is not yet understood. Here we provide a plausible explanation of these phenomena based on the changes in the phase stability of Pb-Sn solders. *Ab initio*-aided CALPHAD modeling is utilized to translate the electric current-induced effect into the excess Gibbs free energies of the phases. Hence, the phase equilibrium can be shifted by current stressing. The Pb-Sn phase diagrams with and without current stressing clearly demonstrate the change in the phase stabilities of Pb-Sn solders under current stressing.

Soldering is one of the oldest metallurgical processes in human history. It was first carried out as early as 5000 years ago in Mesopotamia[1]. Today, state-of-the-art soldering technologies meet the new challenges of modern applications in electronics, such as 3D-IC interconnections and flip-chip packaging[2]. One common feature of these applications is that the solder joints not only serve as mechanical bridges but also provide electrical interconnections. Both signals and electric power for electronic devices rely on the conducting joints. As an electric current passes through a solder join, it has various effects on it, including thermoelectric and electro-migration effects. The former usually raises the temperature of typical solder joints by the Joule heating. The latter is generally accepted as a purely kinetic process, which may either accelerate or retard the motion of the metallic atoms via the momentum transfer mechanism, under so-called "electron wind forces"[3,4]. Although these effects may occur simultaneously and are normally coupled with each other, the exothermic effect can be compensated for in carefully designed isothermal experiments[5]. In such a case, the phase equilibria of a given alloy are well defined because its thermodynamic states are all controlled.

For advanced and portable electronics applications, the dimensions of solder joints are being reduced while allowing sufficient electric current to pass through them to maintain high functionality. Hence, the current density through each solder joint has increased significantly in the past few decades. Electric currents are therefore having greater effects upon solder joints, and a new physical phenomenon has recently been observed to be induced by an electric current[6–8]. The second phase of the solder gradually dissolves into the matrix phase under current stressing, gradually precipitating back at approximately the same positions when the electric current is turned off. The supersaturation of solders under current stressing with high current densities clearly indicates a change of the phase equilibria; however, the origin of the supersaturation is not yet known. High-Pb solders, which are Pb-Sn alloys that contain over 85 wt.% Pb, are the commonly used high-temperature solders. In this study, the phase stabilities of Pb-Sn binary alloys with and without current stressing are determined by performing *ab initio* calculations and *ab initio*–aided CALPHAD thermodynamic modeling. The thermodynamic foundation of supersaturation under current stressing is elucidated.

Results

The electromigration effect has been considered to be a kinetic process of momentum transfer in which metallic atoms migrate under the influence of the electron wind force[3,4]. Direct evidence of Sn whisker formation at the

anode side and void formation at the cathode side supports this theory very strongly[9]. However, the electromigration effect also induces some complicated phenomena, e.g. Sn whisker formation[9], "electrorecrystallization"[10] and "grain rotation"[11], those are considered in terms of energy as stabilization processes in the study. To estimate the energetic contributions caused by application of an electric current, the corresponding growth rates of Sn whiskers of Sn stripes under current stressing and mechanical compression reported in literature were compared; that is the Sn whisker growth rates under current stressing with a current density of 10^5 A/cm^2 are approximately the same as those of Sn stripes under a compressive stress of 8.75×10^8 Pa[9,12]. Although the only mechanical stress that may be induced by the electromigration effect is the back stress due to externally structural constraints[13], the electromigration-induced excess Gibbs free energy of a certain phase under current stressing can be obtained based on the effective stress. The molar Gibbs free energy of each phase can be described according to Eq. (1):

$$G_m^\alpha = {}^oG_{ref.}^\alpha + {}^{id}G_m^\alpha + {}^{ex}G_m^\alpha + {}^{EM-ex}G_m^\alpha, \quad (1)$$

where ${}^oG_{ref.}^\alpha$, G_m^α, ${}^{id}G_m^\alpha$, ${}^{ex}G_m^\alpha$, ${}^{EM-ex}G_m^\alpha$ are the reference energy of the constituent components, and the molar Gibbs free energy, ideal mixing Gibbs free energy, excess Gibbs free energy due to non-ideal mixing, and excess Gibbs free energy due to the electromigration effect of the solution phase α, respectively.

The alloying effect of the excess Gibbs free energies that are induced by the electromigration effect can be estimated from the empirical characteristic parameter, effective charge, z^*, of the constituent elements, according to Eq. (2)[3,4]:

$$F = z^* eE, \quad (2)$$

where F, e, and E are the combined forces that are exerted on the metallic atoms by the electron wind force and electrostatic force, elementary electric charge, and the electric field, respectively. Since the effective charges of pure Pb and pure Sn are reported to be -50 and -7, respectively[4], the net forces that are induced by application of an electric current exerted on the Pb and Sn atoms of the Pb-Sn binary alloys can be assumed to have a ratio of 7 : 1. Therefore, the corresponding effective stress on Pb atoms can be estimated to be 6.13×10^9 Pa at a current density of 10^5 A/cm^2. The effective stresses on the Pb-Sn alloys were then approximated as linear interpolations of the estimated effective stresses on pure Pb and pure Sn. Doing so assumed uniform current stressing or, equivalently, an absence of the current crowding effect[14].

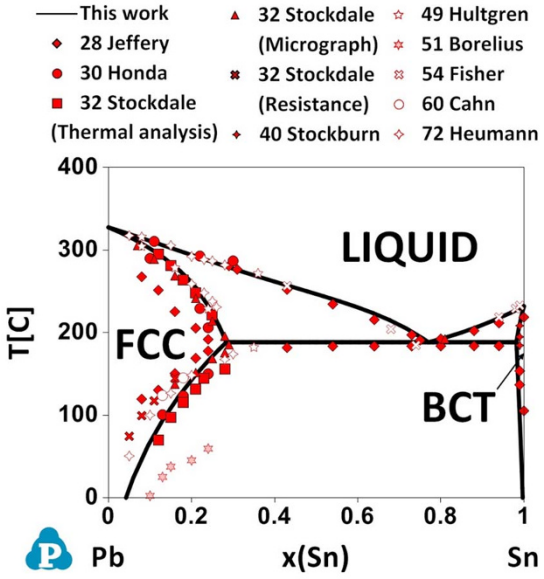

Figure 1 | *Ab initio*-aided CALPHAD calculated Pb-Sn binary phase diagrams without current stressing and with experimental data[15–23] superimposed.

As presented in Fig. 1, the Pb-Sn binary system is a simple eutectic system, which comprises three condensed phases - the liquid phase, the Pb-rich face-centered cubic (FCC) phase, and the Sn-rich body-centered tetragonal (BCT) phases. The *ab initio*-aided CALPHAD calculated phase diagram agrees closely with various experimental data obtained without current stressing[15–23]. Figure 2 shows the *ab initio*-aided CALPHAD calculated Pb-Sn binary phase diagrams under current stressing with various current densities. Please see the supplemental information for the details of the thermodynamic modeling. The phase boundaries of the FCC and BCT phases are indeed shifted by current stressing at a current density of greater than the critical value of approximately 2.5×10^4 A/cm^2. As the current density increases, the Sn solubility in the FCC phase increases, while the Pb solubility in the BCT phase decreases. This trend agrees excellently with experimental results[6,7]. Although solders have been used for thousands of years, the electric current-induced phase transformation was only discovered very recently, probably because the phase transformation can only be triggered when the current density is as high as it must be in modern applications. Moreover, the two peculiar experimental observations could be comprehended according to Fig. 2: (1) under current stressing, the gradual disappearance of the BCT phase is the result of the increasing solubility of Sn in the FCC phase, and (2) the "ring-shape" morphology of the BCT phase during the disappearance of that phase under current stressing is transient as the BCT phase dissolves into the FCC phase and the FCC phase simultaneously precipitates within the BCT phase. (See ref. 4 and the supplemental information for more information.)

Discussion

As illustrated in Fig. 3, under current stressing, "supersaturation" of the FCC phase (disappearance of the BCT phase), "undersaturation" of the BCT phase (precipitation of the FCC phase from the BCT phase), or both simultaneously are expected. The five possible cases depend on the nominal compositions of the Pb-Sn alloys: (1) in the single FCC phase region with or without current stressing, no phase transformation occurs; (2) in the region which is the FCC + BCT two-phase region without current stressing and the single FCC phase region with current stressing, Sn dissolves into the FCC phase and the FCC phase simultaneously precipitates from the BCT phase, forming

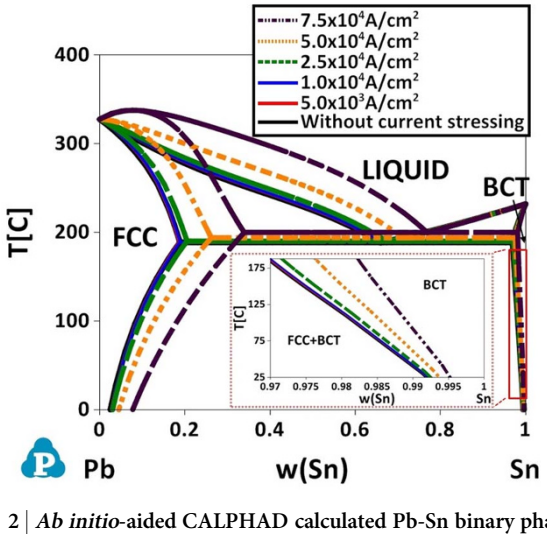

Figure 2 | *Ab initio*-aided CALPHAD calculated Pb-Sn binary phase diagrams without and with current stressing with respect to the current densities of 5.0×10^3, 1.0×10^4, 2.5×10^4, 5.0×10^4, and 7.5×10^4 A/cm^2.

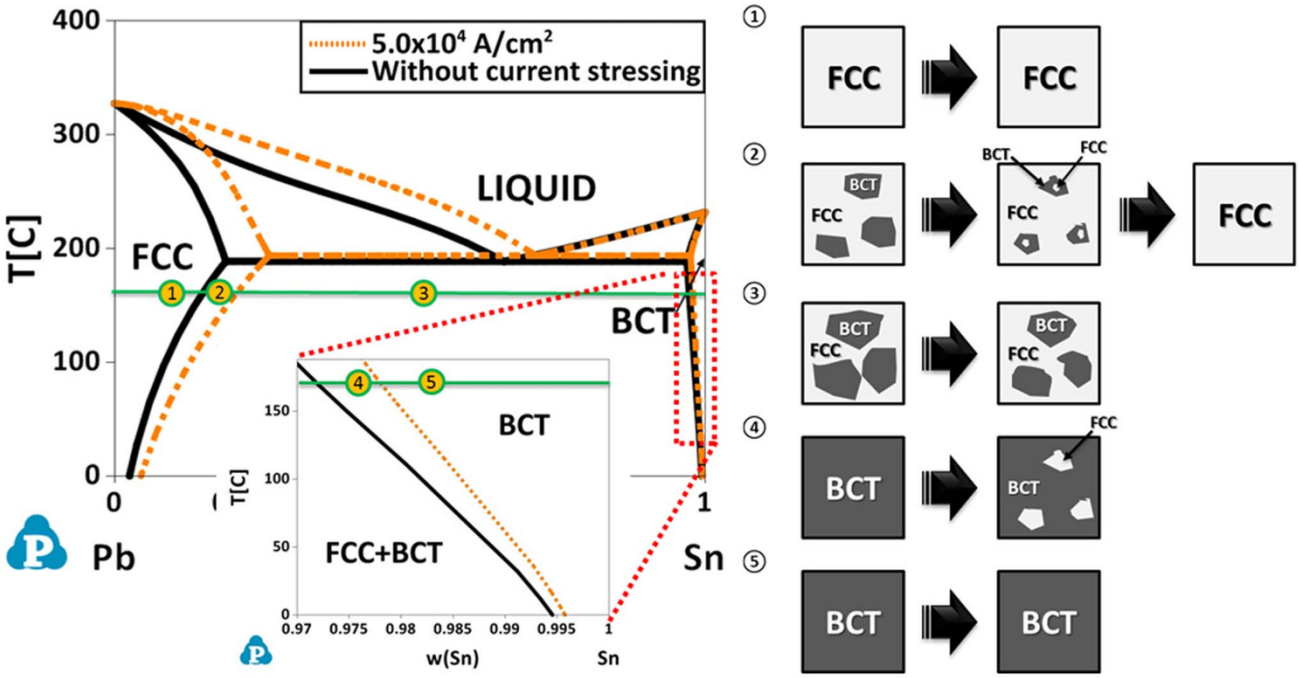

Figure 3 | **Schematic diagrams of the microstructural evolutions of the Pb-Sn alloys under current stressing.**

FCC-BCT core-shell grains as a transient state, and eventually forming a single FCC phase; (3) in the FCC + BCT two-phase region with or without current stressing, the phase fraction of the two phases changes; (4) in the region which is the single BCT phase region without current stressing and the FCC + BCT two-phase region with current stressing, the FCC phase precipitates from the BCT phase; (5) in the single BCT phase region with or without current stressing, no phase transformation occurs.

To examine the effects of current density and temperature upon phase stability under current stressing, the extent of "supersaturation" or "undersaturation" is defined as the saturability, ζ:

$$\zeta = \frac{c_1 - c_0}{c_0} \times 100\%. \quad (3)$$

where c_0, and c_1 are the solubility in the absence and presence current stressing, respectively. Figure 4 plots the saturabilities of both Sn in FCC and Pb in BCT against temperature. The positive and negative values correspond to the "supersaturation" and "undersaturation," respectively. Higher current densities induce larger shifts of equilibria. Furthermore, the extent of "supersaturation" of the FCC phase decreases as temperature increases, while the extent of "undersaturation" of the BCT phase remains nearly unchanged at temperatures from 25 to 180°C.

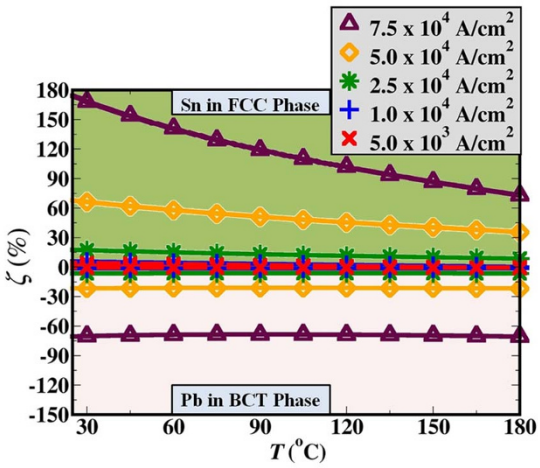

Figure 4 | **Saturabilities of Sn in the Pb-rich FCC phase (upper half) and Pb in the Sn-rich BCT phase (lower half) of the Pb-Sn binary system at temperatures from 25 to 180°C.**

In summary, the thermodynamic foundation of the changing of solder stabilities under current stressing – a newly observed physical phenomenon – is clarified. The electromigration-induced excess enthalpies of the phases shift the phase equilibria of the solders. The calculations herein reveal that the phenomenon occurs only when the current density exceeds the critical value for a particular system and becomes severer as the current density increases. However, similar effects in other solders, including various Pb-free solders, which are currently of interest for eliminating environmental contamination, should be considered. We hope that the present study will open up an avenue of research into the effects of current on the phase stabilities of such solders.

Methods

The zero-Kelvin formation energies of the two solid phases in the Pb-Sn binary system, the FCC and BCT phases, are calculated using the Vienna Ab-initio Simulation Package (VASP)[24] and the density functional theory (DFT) with a plane wave basis. The generalized gradient approximation (GGA) exchange-correlation functional, parameterized by Perdew-Burke-Ernzerhof (PBE)[25] and the projector augmented wave (PAW) method[26] with an energy cut-off of 150 eV, were used. In this work, 32-atom special quasirandom structures (SQSs) of binary FCC structures were taken from Pezold *et al.*[27], while the SQSs of binary BCT structures were constructed herein from 32 atoms using the alloy theoretic automated toolkit (ATAT)[28]. The *k*-point meshes for Brillouin zone sampling were constructed using the Monkhost-Pack scheme[29] and $10 \times 10 \times 10$ and $12 \times 12 \times 10$ *k*-point meshes were used with the 32-atom FCC and BCT cells, respectively. The numerical integration of the Brillouin zone and the energy cut-off were verified to produce an absolute energy convergence of better than 10^{-3} eV/atom, with the convergence of forces at each atomic site to within 10^{-2} eV/Å. The excess entropies in the Gibbs free energy models of the FCC and BCT phases were optimized according to all available experimental information using the CALPHAD method with the PanOptimizer module of the PANDAT software[30]. The phase diagrams of the Pb-Sn binary system with and without current stressing were calculated using the PanPhaseDiagram module of the PANDAT software.

1. George, B., Henry, C. & John, V. *Materials Handbook.* 768–770 (McGraw Hill, New York, 1996).
2. Tu, K. N. Reliability challenges in 3D IC packaging technology. *Microelectron. Reliab.* **51**, 517–523 (2011).
3. Huntington, H. B. & Grone, A. R. Current-induced marker motion in gold wires. *J. Phys. Chem. Solids.* **20**, 76–87, doi:http://dx.doi.org/10.1016/0022-3697(61)90138-x (1961).
4. Lloyd, J., Tu, K.-N. & Jaspal, J. The physics and materials science of electromigration and thermomigration in solders. *Handbook of Lead-Free Solder Technology for Microelectronic Assemblies.* Karl J. Puttliz & Kathleen A. Stalter (ed.), (CRC Press, New York, 2004).
5. Chen, S. W., Chen, C. M. & Liu, W. C. Electric current effects upon the Sn/Cu and Sn/Ni interfacial reactions. *J. Electron. Mater.* **27**, 1193–1198, doi:http://dx.doi.org/10.1007/s11664-998-0068-5 (1998).
6. Chiu, Y.-T., Liu, C.-H., Lin, K.-L. & Lai, Y.-S. Supersaturation induced by current stressing. *Scripta. Mater.* **65**, 615–617, doi:http://dx.doi.org/10.1016/j.scriptamat.2011.06.041 (2011).
7. Chiu, Y. T., Lin, K. L. & Lai, Y. S. Dissolution of Sn in a SnPb solder bump under current stressing. *J. Appl. Phys.* **111**, 043517, doi:http://dx.doi.org/10.1063/1.3682480 (2012).
8. Chen, W.-Y. *et al.* Anisotropic dissolution behavior of the second phase in SnCu solder alloys under current stress. *Scripta. Mater.* **68**, 317–320 (2013).
9. Liu, C. Y., Chen, C. & Tu, K. N. Electromigration in Sn-Pb solder strips as a function of alloy composition. *J. Appl. Phys.* **88**, 5703–5709, doi:http://dx.doi.org/10.1063/1.1319327 (2000).
10. Chiu, Y.-T. *et al.* Electrorecrystallization of metal alloy. *J. Alloy. Compd.* **549**, 190–194, doi:http://dx.doi.org/10.1016/j.jallcom.2012.08.138 (2013).
11. Wu, A. T., Gusak, A. M., Tu, K. N. & Kao, C. R. Electromigration-induced grain rotation in anisotropic conducting beta tin. *Appl. Phys. Lett.* **86**, 241902, doi:http://dx.doi.org/10.1063/1.1941456 (2005).
12. Tu, K. N. Irreversible-processes of spontaneous whisker growth in bimetallic Cu-Sn thin-film reactions. *Phys. Rev. B* **49**, 2030–2034, doi:http://dx.doi.org/10.1103/PhysRevB.49.2030 (1994).
13. Gan, H. & Tu, K. N. Polarity effect of electromigration on kinetics of intermetallic compound formation in Pb-free solder V-groove samples. *J. Appl. Phys.* **97**, 063514, doi:http://dx.doi.org/10.1063/1.1861151 (2005).
14. Tu, K. N. Recent advances on electromigration in very-large-scale-integration of interconnects. *J. Appl. Phys.* **94**, 5451–5473, doi:http://dx.doi.org/10.1063/1.1611263 (2003).
15. Jeffery, F. H. The lead-tin system of alloys re-examined by an electrical resistance method. *T. Faraday Soc.* **24**, 209–215 (1928).
16. Honda, K. & Abe, H. On the equilibrium diagram of the lead-tin System. *Sci. Rep.* **19**, 315–330 (1930).
17. Stockdale, D. The constitution of the lead-tin alloys. *J. Inst. Metals* **49**, 267–286 (1932).
18. Stockburn, A. The solubility of lead in tin. *J. Inst. Metals* **66**, 33–38 (1940).
19. Hultgren, R. & Lever, S. A. Use of electrical resistance measurements to determine the solidus of the lead-tin system. *Trans. AIME* **185**, 67–71 (1949).
20. Borelius, G. Kinetics of precipitation in supercooled solid solutions. *Trans. AIME* **191**, 477–484 (1951).
21. Fisher, H. J. & Phillips, A. Viscosity and density of liquid lead-tin and antimony-cadmium alloys. *Trans. AIME* **200**, 1060–1070 (1954).
22. Cahn, J. W. & Treaftis, H. N. The solubility of tin in solid lead. *Trans. AIME* **218**, 376–377 (1960).
23. Heumann, T. & Wostmann, H. Thermodynamic data for lead-tin alloys and hypothetical transformation of tetragonal tin into face-centered cubic modification. *Z. Metallkd.* **63**, 332–341 (1972).
24. Kresse, G. & Furthmüller, J. Efficient iterative schemes for ab initio total-energy calculations using a plane-wave basis set. *Phys. Rev. B* **54**, 11169–11186 (1996).
25. Perdew, J. P., Burke, K. & Ernzerhof, M. Generalized gradient approximation made simple. *Phys. Rev. Lett.* **77**, 3865–3868 (1996).
26. Blöchl, P. E. Projector augmented-wave method. *Phys. Rev. B* **50**, 17953–17979 (1994).
27. von Pezold, J., Dick, A., Friák, M. & Neugebauer, J. Generation and performance of special quasirandom structures for studying the elastic properties of random alloys: application to Al-Ti. *Phys. Rev. B* **81**, 094203, doi:http://dx.doi.org/10.1103/PhysRevB.81.094203 (2010).
28. van de Walle, A., Asta, M. & Ceder, G. The alloy theoretic automated toolkit: a user guide. *Calphad* **26**, 539–553, doi:http://dx.doi.org/10.1016/s0364-5916(02)80006-2 (2002).
29. Monkhorst, H. J. & Pack, J. D. Special points for Brillouin-zone integrations. *Phys. Rev. B* **13**, 5188–5192 (1976).
30. Cao, W. *et al.* PANDAT software with PanEngine, PanOptimizer and PanPrecipitation for multi-component phase diagram calculation and materials property simulation. *Calphad* **33**, 328–342 (2009).

Acknowledgements

The authors gratefully acknowledge the financial support from the National Science Council (NSC) in Taiwan (NSC101-2221-E-006-113). S.K.L. and M.Y. are thankful to the support to PCGMR from NCKU headquarter, the President Hwung-Hweng Hwung, the Dean Pao-Shan Yu, and Department Chairs Jyh-Ming Ting and Jiunn-Der Liao. Ted Knoy is appreciated for his editorial assistance.

Author contributions

S.K.L. conceived and directed the research. C.K.Y. and W.X. constructed the SQSs of the BCT structure. C.K.Y. and Y.C.L. performed the *ab initio* calculations and CALPHAD thermodynamic modeling. S.K.L. and M.Y. supervised the calculations and contributed to manuscript preparation. All authors discussed the results and implications and commented on the manuscript at all stages.

Additional information

Supplementary information accompanies this paper at http://www.nature.com/scientificreports

Competing financial interests: The authors declare no competing financial interests.

How to cite this article: Lin, S., Yeh, C., Xie, W., Liu, Y. & Yoshimura, M. *Ab initio*-aided CALPHAD thermodynamic modeling of the Sn-Pb binary system under current stressing. *Sci. Rep.* **3**, 2731; DOI:10.1038/srep02731 (2013).